Vision Research 51 (2011) 1760–1766

Contents lists available at ScienceDirect

Vision Research

journal homepage: www.elsevier.com/locate/visres

Global shape processing involves a hierarchy of integration stages

Jason Bell [a,b,*], Elena Gheorghiu [c], Robert F. Hess [a], Frederick A.A. Kingdom [a]

[a] McGill Vision Research, Dept. of Ophthalmology, McGill University, 687 Pine Av. West, H4-14, Montreal, Quebec, Canada H3A 1A1
[b] Dept. of Psychology, Australian National University, Canberra, ACT 0200, Australia
[c] Laboratory of Experimental Psychology, University of Leuven, Tiensestraat 102, B-3000 Leuven, Belgium

ARTICLE INFO

Article history:
Received 24 January 2011
Received in revised form 20 April 2011
Available online 16 June 2011

Keywords:
Contour
Curvature
Orientation
Adaptation
Shape

ABSTRACT

Radial Frequency (RF) patterns can be used to study the processing of familiar shapes, e.g. triangles and squares. Opinion is divided over whether the mechanisms that detect these shapes integrate local orientation and position information directly, or whether local orientations and positions are first combined to represent extended features, such as curves, and that it is local curvatures that the shape mechanism integrates. The latter view incorporates an intermediate processing stage, the former does not. To differentiate between these hypotheses we studied the processing of micro-patch sampled RF patterns as a function of the luminance polarity of successive elements on the contour path. Our first study measures shape after effects involving suprathreshold amplitude RF shapes and shows that alternating the luminance polarity of successive micro-patch elements disrupts adaptation of the global shape. Our second study shows that polarity alternations also disrupt sensitivity to threshold-amplitude RF patterns. These results suggest that neighbouring points of the contour shape are integrated into extended features by a polarity selective mechanism, prior to global shape processing, consistent with the view that for both threshold amplitude and suprathreshold amplitude patterns, global processing of RF shapes involves an intermediate stage of processing.

1. Introduction

The detection and recognition of objects is critical to vision and the visual coding of shape is an important part of this process. It is widely acknowledged that the human visual system contains specialised shape detectors (Hayworth & Biederman, 2006; Kourtzi & Kanwisher, 2001; Lerner, Hendler, Ben-Bashat, Harel, & Malach, 2001; Wilkinson et al., 2000). In order to encode the outline shape of an object a mechanism must spatially integrate information from various points along the outline. The aim of this study is to determine whether this mechanism directly integrates local position and/or orientation information along the contour, or whether there is an intermediate stage, or stages, in which neighbouring orientations and/or positions are first pooled to represent curves, which are then integrated to represent the whole shape, as suggested in some recent models of global shape coding (Poirier & Wilson, 2006, 2010).

Traditionally, line drawings of objects have been used to determine which parts of a contour outline are important for representing shape, and points deviating from a straight line have been deemed the most important (Attneave, 1954; Biederman, 1987; De Winter & Wagemans, 2006; Hoffman & Richards, 1984; Hoffman & Singh, 1997; Koenderink & van Doorn, 1982). In order to understand how the visual system encodes points of deviation it would seem prudent to use stimuli that allow the local features of a shape to be parametrically varied. For this reason, several researchers have employed Radial Frequency or, RF patterns to study holistic shape processing (Bell, Wilkinson, Wilson, Loffler, & Badcock, 2009; Hess, Achtman, & Wang, 2001; Jeffrey, Wang, & Birch, 2002; Kurki, Saarinen, & Hyvarinen, 2009; Mullen & Beaudot, 2002; Wilkinson, Wilson, & Habak, 1998). RF patterns are created by sinusoidally modulating the radius of a circle (see Fig. 1) and their design affords precise control of the information at each point on the contour as well as the overall shape. The number of full cycles of modulation per 2π radians is the RF number, and by changing this number the pattern assumes simple shapes such as triangles (RF3), squares (RF4) and pentagons (RF5). Changing the phase of the modulation varies the orientation of the shape, e.g. a square or diamond. By summing different RF modulations with particular phases and modulation amplitudes, RF patterns can also be used to study more complex object shapes such as fruit and human body parts (Loffler, 2008; Poirier & Wilson, 2010; Wilkinson, Shahjahan, & Wilson, 2007; Wilson & Wilkinson, 2002; Wilson, Wilkinson, Lin, & Castillo, 2000).

Studies measuring the *detection* of RF shapes, namely the threshold amplitude for discriminating an RF pattern from a circle, have for the most part shown that information is integrated around the whole contour (Bell & Badcock, 2008, 2009; Hess, Wang, &

* Corresponding author at: Dept. of Psychology, Australian National University, Canberra, ACT 0200, Australia.
E-mail address: Jason.Bell@anu.edu.au (J. Bell).

0042-6989/$ - see front matter Crown Copyright © 2011 Published by Elsevier Ltd. All rights reserved.
doi:10.1016/j.visres.2011.06.003

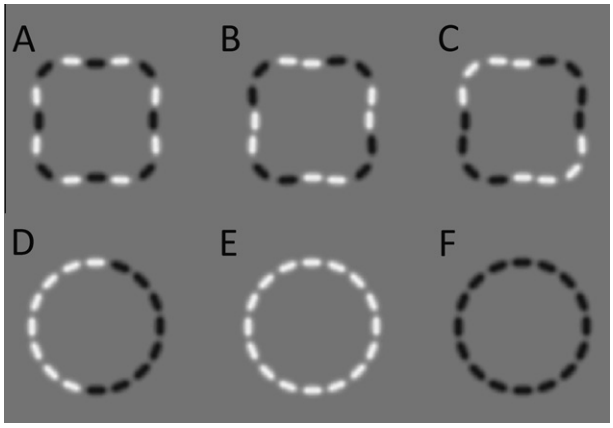

Fig. 1. Example RF4 stimuli used in this study. (A–F) Examples of the different luminance polarity conditions. From (A–F) the frequency of the luminance polarity alternations in each pattern is halved, culminating in all white elements (E) or all dark elements (F). (A–C) RF4 stimuli at amplitudes of 0.15. (D–F) RF4 stimuli with no modulation amplitude (circles).

Dakin, 1999; Jeffrey et al., 2002; Loffler, Wilson, & Wilkinson, 2003; Wilkinson et al., 1998); although see Mullen, Beaudot, and Ivanov (2011). While the argument that RF detection involves whole-shape encoding is generally agreed upon, there is disagreement as to which local features are integrated. Three features are potentially available: (a) local orientations, which are maximally different at the zero-crossings of the modulation function; (b) local positions, which are maximally different at the peaks and troughs of the function, and (c) curvatures, which vary in both magnitude and sign around the shape. Curvature can be considered a higher order feature in that it is computed from the combination of local orientations and/or positions along the contour (Bell, Badcock, Wilson, & Wilkinson, 2007; Gheorghiu & Kingdom, 2009; Hancock & Peirce, 2008; Poirier & Wilson, 2006, 2007).

Some researchers have argued that for RF detection, neighbouring orientation and position signals are first integrated to encode local curves, and then the curves are integrated to encode the RF shape (Bell, Dickinson, & Badcock, 2008; Bell & Kingdom, 2009; Habak, Wilkinson, & Wilson, 2006; Habak, Wilkinson, Zakher, & Wilson, 2004; Poirier & Wilson, 2006, 2007; Wilkinson et al., 1998). Although this view is consistent with some neurophysiological models of shape representation (Carlson, Rasquinha, Zhang, & Connor, 2011; Connor, 2004; Muller, Wilke, & Leopold, 2009; Pasupathy & Connor, 2002; Yamane, Carlson, Bowman, Wang, & Connor, 2008), there is little direct evidence that curvature constitutes an intermediate feature in RF detection. Indeed, other researchers have argued that local orientations and positions are directly integrated for detecting RF shapes (Hess et al., 1999; Jeffrey et al., 2002; Mullen & Beaudot, 2002; Wang & Hess, 2005).

What type of local feature information is involved in the representation of *suprathreshold* RF shapes? No studies have directly addressed this question, despite the fact that in order to accurately represent simple shapes such as triangles and squares, or complex shapes such as fruit and head shapes, RF patterns must be presented at suprathreshold amplitudes (Bell & Kingdom, 2009; Wilkinson et al., 1998; Wilson et al., 2000). Therefore it is important to understand how suprathreshold amplitude RF patterns are processed, and recent studies have confirmed that it does involve the integration of local feature information (Bell, Hancock, Kingdom, & Peirce, 2010; Bell & Kingdom, 2009). However, although Day and Loffler (2009) have shown that both orientation and position features are used for representing suprathreshold RF patterns, the question remains as to whether there are intermediate stages involved. In short, we wish to know whether suprathreshold RF processing involves intermediate-stage mechanisms, such as those sensitive to curvature.

Thus we aim to decide between two hypotheses: (1) that local orientations and/or positions are the primitive features that are integrated for representing global shape, or (2) that global shape coding includes an intermediate stage, or stages, that integrate adjoining local orientation and position information into more complex features, such as curves, prior to encoding global shape. We use micro-patch-sampled RF patterns (see Fig. 1) to examine both threshold amplitude and suprathreshold amplitude RF shapes. Experiment 1 uses an appearance-based measure – the after-effect of RF amplitude resulting from adaptation (Bell & Kingdom, 2009) – applied to suprathreshold amplitude RFs, with the aim of examining the nature of the interactions between neighbouring orientation and position features. Experiment 1 shows that alternating the luminance polarity of the elements in the adaptor RF severely disrupts the after-effect induced in a single-polarity RF test, but when the adaptor elements are re-ordered to produce strings of same-polarity elements, the disruption is reduced in proportion to the length of the string. Experiment 2 aims to test whether the disruptive effects of luminance polarity alternation on RF processing generalized to threshold amplitudes measured using a performance-based task – RF detection. RF detection thresholds fall significantly as the number of consecutive elements of the same polarity increased. Thus both experiments show a disruptive effect of luminance polarity alternation, and suggest that orientation and position features are integrated into intermediate, more complex feature representations prior to encoding overall shape.

2. Methods

2.1. Participants

Six experienced psychophysical observers participated in the current study. Four were naïve as to the experimental aims, whilst observers J.B. and E.G. were authors. All had normal or corrected-to-normal visual acuity. Participation was voluntary and unpaid.

2.2. Apparatus and stimuli

Stimuli were created using Matlab version 7.6, and loaded into the frame-store of a Cambridge Research Systems (CRS) ViSaGe video-graphics system. Stimuli were presented on a Sony Trinitron G400 monitor with a screen resolution of 768 × 1024 pixels and a refresh rate of 100 Hz. Using this screen resolution in conjunction with a viewing distance of 115 cm resulted in each pixel on the screen subtending 1′ of visual angle. The luminance of the monitor was calibrated using an Optical OP200-E (Head Model # 265). The mean luminance of the monitor was 50.4 cd/m^2.

The adaptation and test stimuli were micro-patch-sampled Radial Frequency (RF) contours (see Fig. 1). The RF contours were created by modulating the radius of a circle using a sinusoidal function

$$r(\theta) = r_{mean}(1 + A\sin(\omega\theta + \varphi)) \quad (1)$$

where r is the radius and θ the angle representing the polar coordinates of the contour, r_{mean} is the average contour radius, A the amplitude of radius modulation (between 0 and 1), ω the RF number (4 in this study) and φ the angular phase (orientation) of the shape. In our study, the shape of the RF4 pattern was represented by 16 oriented micro-patches, four per modulation cycle. For an RF4, 16 is the desirable number of micro-patches as it allows a micro-patch to be positioned either at the locations where orientation changes maximally with amplitude, i.e. the zero-crossings of the

modulation function, or where position changes maximally with amplitude, i.e. at the peaks and troughs of the waveform. Using this stimulus design, each micro-patch changes in only one characteristic, orientation or position, as amplitude is varied, since the eight micro-patches positioned at the zero-crossings vary only in orientation while the eight positioned at the peaks and troughs vary only in position.

The luminance profile perpendicular to the major axis of the micro-patches was a Gaussian envelope with sigma equal to 0.067°. Along the major axis of the micro-patches, the Gaussian envelope had the same sigma but was applied to the outer edge of a circular aperture in order to avoid any distortion of the shape of the luminance envelope as a function of orientation. Fig. 1 shows example RF4 contours and micro-patch components. The luminance contrast of each micro-patch was set to its maximum possible value (+1 for white and −1 for dark).

2.3. Procedure

RFAAEs (Exp. 1): A staircase procedure was employed to measure a Radial Frequency amplitude after-effect, or RFAAE, whereby the perceived amplitude of an RF pattern is shifted by adaptation in a direction away from that of the adaptation amplitude. The procedure was the same as that used by Bell and Kingdom (2009). The adaptation period lasted 1 min, during which the angular phase and position of each RF adapting pattern was independently jittered every 500 ms. This was done to minimise systematic orientation and/or position adaptation relative to the test patterns. The adapting patterns were presented simultaneously 3° above and 3° below the fixation cross. The amplitudes (A in Eq. (1)) of the adapting patterns were 0.05 and 0.15, giving a geometric mean of 0.086. Each cycle of the test period began with a 400 ms blank screen, followed by the test pair for 500 ms (signalled by a tone), then a blank screen of 100 ms and finally 2 s top-up adaptation. The test pair were also presented simultaneously 3° above and 3° below the fixation cross and the observer was instructed to select whether the upper or lower test pattern appeared to be the more deformed from circularity (or the higher in amplitude [A in Eq. (1)]). The angular phase of the test pair was randomly drawn on each trial with a random positional jitter then applied to each pattern individually. The amplitude ratio of the test patterns on the first test trial was set to a random number between 0.5 and 1.5 (upper divided by lower) but with geometric mean amplitude fixed at 0.086. Following each response (a key press) the computer adjusted the ratio of amplitudes in a direction opposite to that of the response, i.e. towards the point of subjective equality (PSE). For the first six trials, the ratio was adjusted by a factor of 1.12, and thereafter by a factor of 1.06. Each run was terminated after 25 trials and the PSE was calculated as the geometric mean ratio of test pattern amplitudes over the last 20 trials, which on average contained 6–10 reversals. Typically, six PSEs were measured for each condition. In half of the sessions, the high amplitude adapting pattern was in the upper visual field whereas in the other half of the sessions the lower amplitude adapting pattern was in the upper visual field. In addition, we measured the PSE in sessions containing no adaptation stimuli; these served as baselines with which to compare the size of the RFAAE with adaptation. The size of the after-effect calculated for each session was given by the log ratio of test amplitudes (corresponding to the lower and higher adapting amplitudes) at the PSE minus the same PSE value without adaptation. The mean and standard error (S.E.) of these values across sessions are the points shown in the graphs.

RF discrimination thresholds (Exp. 2): The threshold for detecting modulation in an RF4 contour was measured using a temporal two-interval forced choice procedure, in which the observer was required to choose the pattern that appeared most deformed from circularity. No feedback was given. The spatial location corresponding to the centre of each pattern was spatially jittered in any direction up to 0.25° about the centre of the screen. No fixation point was provided. The test and reference patterns appeared in random order for 160 ms with a 500 ms ISI. The reference pattern was always a smooth circle ($A = 0$ in Eq. (1) [see Fig. 1E]) while the test pattern had some amount of radius modulation amplitude. The phase of modulation (shape orientation) was randomised on each trial. The method of constant stimuli (MOCS) was used to control stimulus presentation. A logistic function was fit to the data in order to obtain an estimate of the modulation amplitude corresponding to 75% accuracy.

3. Experiments

3.1. Experiment 1: RFAAEs with alternating-polarity strings

To determine whether there are intermediate stages involved in coding suprathreshold RFs we exploited the fact that local curvature processing is known to be luminance-polarity selective (Gheorghiu & Kingdom, 2006). We manipulated the number of consecutive 'white' (positive luminance contrast) and 'dark' (negative luminance contrast) elements on the RF adapting pattern and measured the effect on the RFAAE. The adapting pattern was always represented by 16 elements, but the number of consecutive white elements was either: 1, 2, 4, 8, or 16 (e.g. see Fig. 1A–E). We also tested the luminance polarity selectivity of the RFAAE using an all dark adaptor. In all conditions the test pattern contained 16 white elements. If orientation and position cues directly code global shape, then the exact configuration of the white and dark elements should have no effect on the size of the RFAAE, since changing the ordering of the elements' polarities has no effect on the orientation and position information at each point, or the total number of elements of each polarity. However, if global shape mechanisms integrate neighbouring orientation and position features into intermediate, polarity-specific features prior to global shape integration, RFAAEs should increase with the number of consecutive same-polarity elements.

Fig. 2 (grey columns) shows RFAAEs for five observers as a function of the number of consecutive same-polarity elements along the contour. White and black columns show RFAAEs for an all white (W) and all dark (D) adaptor respectively (in all conditions the test was all white). The bottom right panel in Fig. 2 shows the mean results for all observers in each condition. When the luminance polarity of the adaptor alternated every element (condition 1A) the RFAAE was completely absent. However, RFAAEs systematically increased with the number of consecutive elements of the same polarity, culminating in largest RFAAEs when adaptor and test were represented by all white elements (condition W). The increase across conditions is significant ($F_{(4,16)} = 16.78$, $p < .0001$). Interestingly, RFAAEs did not plateau once the adaptors contained four consecutive elements, as one might expect if the intermediate stage is a simple curvature mechanism sensitive to a half cycle of modulation (Gheorghiu & Kingdom, 2007b, 2008, 2009; Hancock & Peirce, 2008). Instead, RFAAEs continue to rise with number of consecutive same-polarity elements. Finally, when adaptor and test patterns were single-but- opposite polarity (adaptor all dark, test all white, condition D) there was less transfer than when adaptor and test were all white (condition W). We will return to this result in Section 4.

It is clear from these results that polarity alternation disrupts adaptation to the global shape of the RF pattern. This disruption cannot be explained by weak adaptation to dark elements, (remember the test was all white) because conditions involving 1, 2, 4 and 8 consecutive elements all have the same number of dark elements (8) and RFAAEs increase across these conditions.

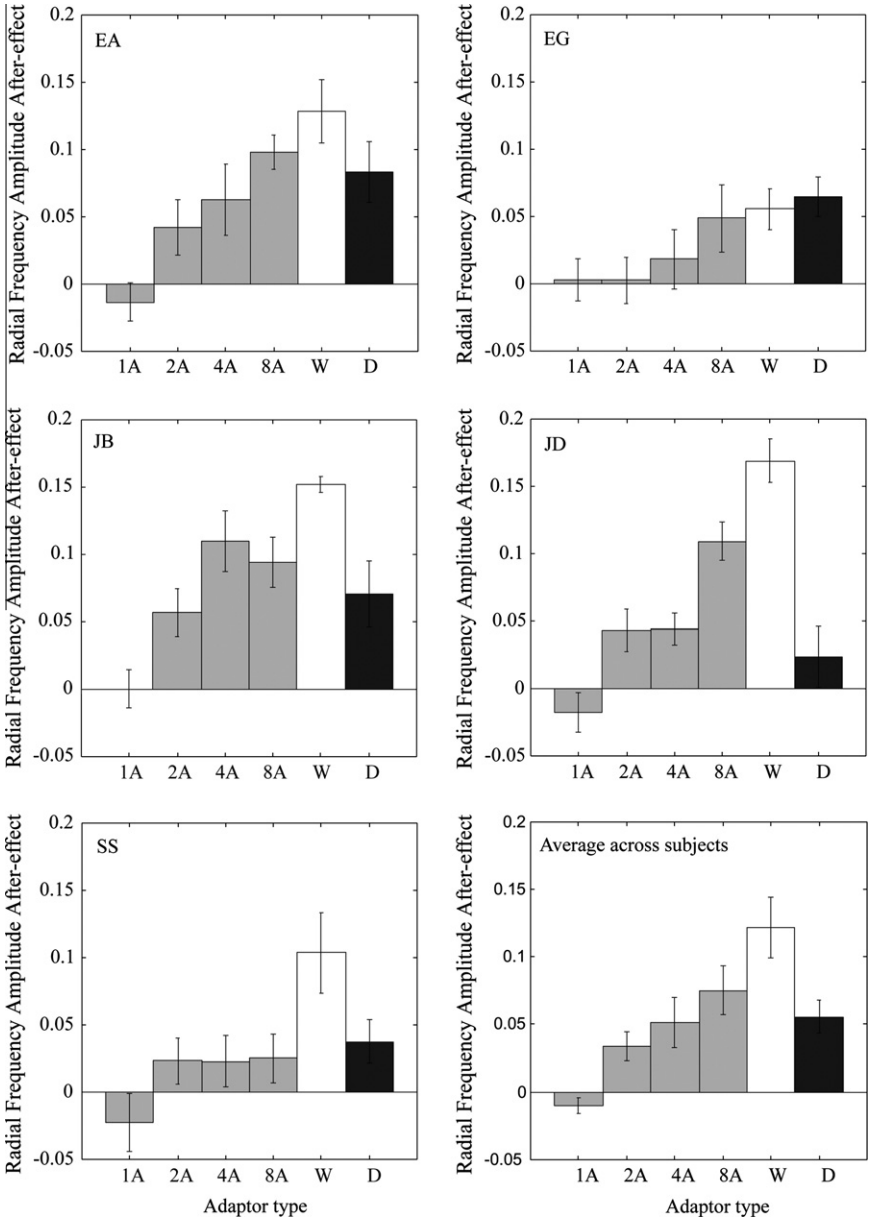

Fig. 2. RFAAEs for five different observers as a function of the number of elements along the path of the adapting pattern that are the same luminance polarity. Vertical axes show the size of the RFAAE on a log scale. Horizontal axes describe the condition: Grey bars indicate conditions where the polarity alternates: (1A) alternating in polarity every other element (Fig. 1A); (2A) alternating in polarity every two elements (Fig. 1B). White bars (labelled W) show RFAAEs for an all white adaptor and black bars (labelled D) for an all dark adaptor. In all cases the test was all white. Error bars here and in other figures throughout the paper show ±1 standard error (S.E.). The bottom right panel shows the average data across observers in each condition.

Fig. 3 shows data for four observers in a control condition in which all the dark elements were removed from the adaptor [see Fig. 3 inset]. This sub-sampled RF pattern yields a strong after-effect; therefore weak adaptation to the dark elements cannot explain our results. Instead the data suggest that optimal global shape adaptation occurs when neighbouring points are of the same luminance polarity, due to the fact that the orientation and position features are combined by intermediate-stage polarity-selective mechanisms.

3.2. Experiment 2: RF detection thresholds with alternating-polarity strings

The majority of the psychophysical literature involving RF patterns has employed performance tasks to measure amplitude thresholds, e.g. (Bell & Badcock, 2009; Dickinson, Almeida, Bell, & Badcock, 2010; Hess et al., 1999; Loffler et al., 2003; Mullen & Beaudot, 2002; Wilkinson et al., 1998). Therefore it seems sensible to ask whether the disruption of suprathreshold RF pattern processing by polarity alternation occurs for threshold RF patterns. If polarity alternations do not disrupt the processing of threshold amplitude patterns then this would imply that the results of Experiment 1 are specific to the choice of stimuli (suprathreshold vs. threshold) and/or procedure (appearance vs. performance) rather than due to a general property of RF shape processing. Therefore we measured RF detection thresholds for the same set of stimuli (see Fig. 1D–F and Section 2).

Fig. 4 shows modulation amplitude thresholds as a function of the number of consecutive same-polarity elements. As with Experiment 1, luminance polarity alternations disrupt the detection of the RF pattern. Apart from the unexpected first data point on the left (the alternating polarity condition), to which we shall return,

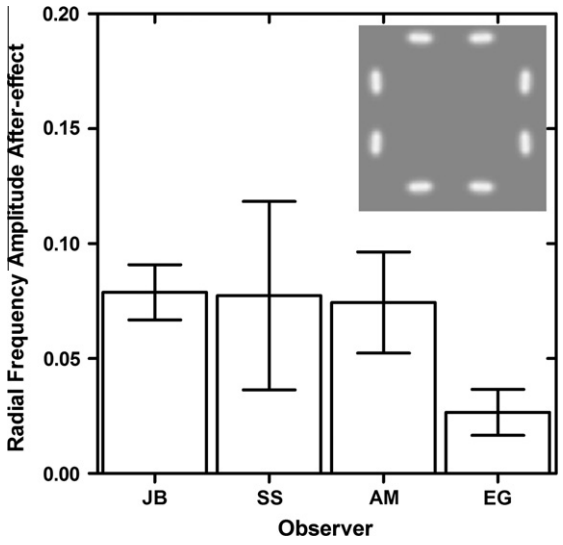

Fig. 3. RFAAEs for four observers in a control experiment in which the eight dark elements of the adapting pattern have been removed. All other aspects of the procedure are identical to those used to obtain RFAAEs in Fig. 2. The inset of figure shows the appearance of the high amplitude adapting RF pattern.

thresholds systematically decrease as the number of consecutive same-polarity elements increases. The decrease in thresholds across conditions is significant ($F_{(4,12)} = 20.31$, $p < .0001$).

4. General discussion

The results of Experiments 1 and 2 show that for both suprathreshold RF patterns measured using an appearance task (Figs. 2 and 3) and threshold amplitude RF patterns measured using a performance task (Fig. 4), polarity alternations disrupt the processing of RF shapes. The disruption is not consistent with the idea that position and orientation information is directly integrated by a global shape mechanism, because if this were true the precise configuration of polarities would not matter. Instead, the number of consecutive elements of the same polarity has a profound influence, suggesting that orientation and position information are combined into intermediate, polarity-selective features prior to global shape encoding. The fact that similar results were obtained under very different experimental protocols makes it unlikely that our findings are an artefact of stimulus or procedure.

Are the intermediate features local curves, i.e. half-cycles of the RF's modulation? We know that contour curvature mechanisms are selective for luminance polarity (Gheorghiu & Kingdom, 2006, 2007a), so our results are consistent with curves being at least one of the intermediate features. The reader can appreciate the importance of local curvature by inspecting Fig. 1A–C. As more elements of a single luminance polarity appear in a chain (A–C), the shape takes on an increasingly curved appearance, despite the physical shape of each pattern being identical. Thus weak adaptation to a shape containing luminance polarity alternations (Fig. 1A) would seem to be consistent with weak curvature adaptation. The reduced sensitivity to modulation in polarity-alternating relative to single polarity RF patterns (Exp. 2, Fig. 4) is also consistent with poor sampling of curvature, assuming that optimal RF sensitivity is underpinned by the detection of a change in curvature, as our own research (Figs. 2 and 4) and others (Bell et al., 2008; Habak et al., 2004; Loffler et al., 2003; Poirier & Wilson, 2007) suggests.

Yet local curvature cannot be the only intermediate feature involved. RFAAEs did not plateau with four consecutive luminance polarity elements (Fig. 2), so optimal RF shape processing appears to involve the integration of intermediate features that extend

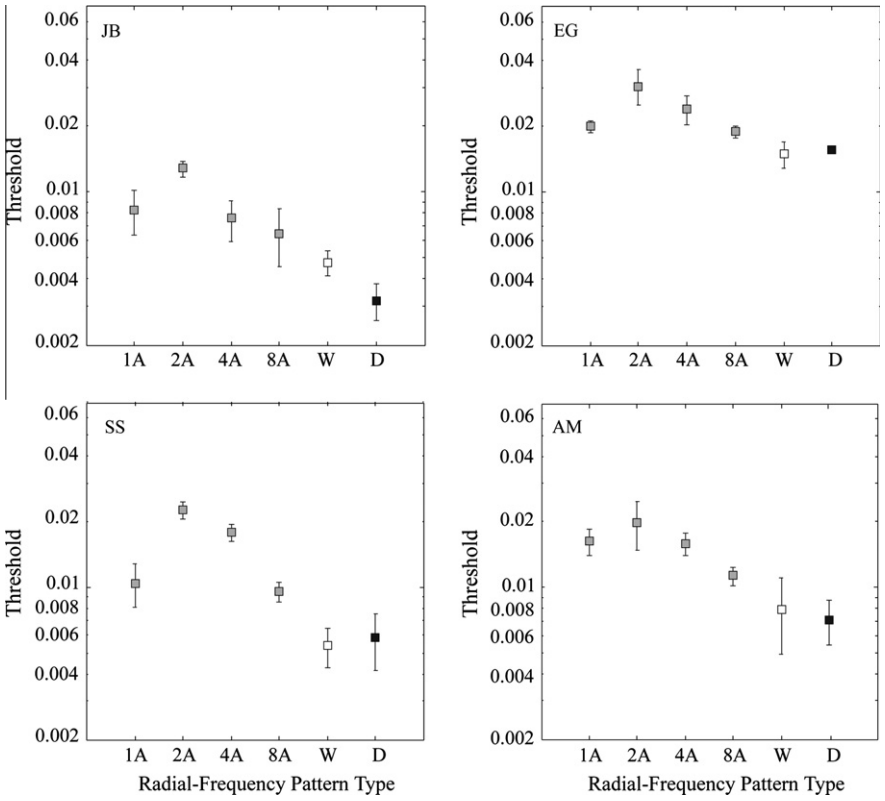

Fig. 4. RF4 discrimination thresholds for four observers as a function of the number of elements along the path that are the same luminance polarity. The vertical axes plot the threshold as a proportion of the mean radius of the test pattern (set at 1°). The description of the conditions on the horizontal axes is the same as described in Fig. 2.

beyond single curves. Current models of RF detection, e.g. Poirier and Wilson (2006), assume that RF patterns are detected by integrating only points of maximum *convex* curvature. For representing suprathreshold amplitude shapes, points of maximum *concave* curvature appear also to be used (Bell, Hancock, et al., 2010). The present results suggest that integration is not restricted to local curvature (concave or convex) but includes a series of intermediate shapes of varying complexity. This conclusion is consistent with recent neurophysiology: Pasupathy and Connor (1999, 2001) have found neurons in macaque area V4 not only selective for curves with particular orientations, positions and degrees of curvature, but also selective for more complex contour configurations, for example contours containing more than one type of curve. Neurons with this type of selectivity have also been found in the posterior inferotemporal cortex (PIT) (Brincat & Connor, 2004, 2006; Yau, Pasupathy, Brincat, & Connor, 2010).

One might be tempted to proffer an explanation for these results in terms of the "association field" advanced to account for results in path detection studies (Field, Hayes, & Hess, 1993). The association field is a putative network of neural facilitation that enhances the signals from elements that form collinear or near-collinear contours. The argument might go that if collinear facilitation were polarity-specific the enhancement would be strongest amongst consecutive same-polarity elements in an RF contour. If one then supposed that only the signal-enhanced elements were input to contour-shape mechanisms, the results of the present study would be predicted. However, a number of considerations make an association-field explanation, at least as presently conceived, unlikely. First, alternating the luminance polarity of consecutive elements along the path in the path-detection paradigm has only a modest effect on performance (Field, Hayes, & Hess, 2000; Field et al., 1993), whereas for the RF patterns here it is highly disruptive, even in the absence of any background clutter. Second, the association field is invoked as a mechanism for enhancing the detection of collinear or near-collinear strings set amongst clutter. Contour-shape mechanisms on the other hand exist to encode a wide range of curvatures including sharp angles, as well as more complex shapes such as those containing inflexions (Bell, Hancock, et al., 2010; Bell, Sampasivam, McGovern, & Kingdom, 2010; Motoyoshi & Kingdom, 2010; Pasupathy & Connor, 1999, 2001), and it is a reasonable assumption that this rich variety of neural architecture is involved in encoding the curvatures and inflexions in the RF patterns used here. Thus whatever non-linearities are involved in combining signals from the elements of RF patterns into intermediate shapes (e.g. multiplication for curvature – see Gheorghiu and Kingdom (2009)), they likely subserve a much wider range of curvatures and shapes than does the association field.

The most likely explanation of the present results is that the shapes of RF patterns are encoded via a hierarchy of shape-sensitive mechanisms for which the intermediate stages are polarity-selective. Of course ours is not the first study to suggest that features other than simple curves are involved in representing shapes. For example, recent research by some of us has shown that in addition to local curvature, the inflection points of a contour outline are used to encode shape (Bell, Hancock, et al., 2010; Bell, Sampasivam, et al., 2010).

Studies of global form processing using Glass patterns (1969) have also reported weak integration of signal elements when successive dipoles are of opposite luminance polarity (Badcock, Clifford, & Khuu, 2005; Or, Khuu, & Hayes, 2007; Wilson, Switkes, & De Valois, 2004), and current models of RF pattern processing (Poirier & Wilson, 2006, 2010) propose that the encoding of RF shapes (Wilkinson et al., 1998) and of Glass patterns (1969) involves a common first stage of orientation processing. However, psychophysical data show that RF patterns and Glass patterns are processed by independent global form mechanisms (Badcock, Almeida, & Dickinson, 2006); therefore both lines of research are important for understanding how global form is processed by the visual system.

Three further aspects of our data warrant discussion. The first relates to the lack of any adaptation transfer from an RF pattern defined by alternating white and dark elements to an all-white test (Fig. 2 condition 1A). What is so striking about this result is that the RFAAE is not just reduced but completely abolished. Indeed, if the black elements are removed from the alternating-polarity adaptor, a level of RFAAE is restored (Fig. 3), suggesting that the obliteration of the after-effect in the alternating condition is not due to undersampling of the adaptor by each of two, separate, polarity-specific mechanisms. Rather, the alternate black elements appear to *suppress* the RFAAE when the test is an all-white adaptor. This is consistent with the idea that the intermediate shape mechanisms combine inputs in such a way that inputs of opposite luminance polarity tend to cancel.

The finding that alternating polarity adaptors are ineffective for inducing shape after-effects in single-polarity tests must however be squared against the result when adaptor and test are both single but of opposite polarity. If the shape-phases of adaptor and test are fixed and equal, there is almost complete transfer of the RFAAE between opposite-polarity adaptors/tests [Figs. 2 and 4B (Bell & Kingdom, 2009)]. In other words global shape processing under these conditions is agnostic to luminance polarity. Moreover, this does not appear to be a result of any undue influence of local orientation adaptation, which is known to be polarity non-specific (Magnussen & Kurtenbach, 1979), since the effect survives a change in RF radius when going from adaptor to test (Bell & Kingdom, 2009). There would thus appear to be an inconsistency between the results of the present study in which single-polarity *random shape-phase* RF shapes show polarity selectivity (Fig. 2 black bars), and the results of our previous study with single-polarity, *fixed shape-phase* RF shapes showing polarity non-selectivity. The discrepancy is resolved however if one posits that luminance polarity is critical when integrating local information to encode a global shape, but that once global shape is encoded, luminance polarity is discarded. Put more simply, with randomized-shape-phase adaptation, the full global shape, which includes its overall orientation, appears not to be encoded and as a result not all polarity information is discarded.

Finally, why in the second experiment were thresholds highest for the pair-alternating rather than single-alternating polarity condition (leftmost data points in Fig. 4)? Inspection of the near-threshold versions of these two conditions in Fig. 1B and A reveals that the pair-alternating condition seems to be the more disruptive. A speculative reason for this is that when going from the alternating to the pair-alternating condition the visual system switches from local orientation/position coding to curvature coding of the RF pattern, but because the curvature information provided by each pair is so impoverished, the resulting signal-to-noise ratio ends up being lower.

In summary, we have presented evidence that orientation and position features are not independently integrated to represent RF patterns, but are first combined into a hierarchy of intermediate shape features that are luminance-polarity selective.

Acknowledgments

This research was supported by the Natural Sciences and Engineering Research Council (NSERC) of Canada, (Grant #OGP01217130) given to F.K., by the Canadian Institute for Health Research (CIHR) (Grant #MT 108-18) given to R.F.H. and by a Research Foundation Flanders (Fonds Wetenschappelijk Onderzoek – Vlaanderen) fellowship given to E.G.

References

Attneave, F. (1954). Some informational aspects of visual perception. *Psychological Review, 61*(3), 183–193.

Badcock, D. R., Almeida, R., & Dickinson, J. E. (2006). Detecting the shape and position of global form: More than one process. *Australian Journal of Psychology, 58*, S62.

Badcock, D. R., Clifford, C. W., & Khuu, S. K. (2005). Interactions between luminance and contrast signals in global form detection. *Vision Research, 45*(7), 881–889.

Bell, J., & Badcock, D. R. (2008). Luminance and contrast cues are integrated in global shape detection with contours. *Vision Research, 48*(21), 2336–2344.

Bell, J., & Badcock, D. R. (2009). Narrow-band radial frequency shape channels revealed by sub-threshold summation. *Vision Research, 49*(8), 843–850.

Bell, J., Badcock, D. R., Wilson, H., & Wilkinson, F. (2007). Detection of shape in radial frequency contours: Independence of local and global form information. *Vision Research, 47*(11), 1518–1522.

Bell, J., Dickinson, J. E., & Badcock, D. R. (2008). Radial frequency adaptation suggests polar-based coding of local shape cues. *Vision Research, 48*(21), 2293–2301.

Bell, J., Hancock, S., Kingdom, F. A. A., & Peirce, J. W. (2010). Global shape processing: Which parts form the whole? *Journal of Vision, 10*(6), 1–13.

Bell, J., & Kingdom, F. A. A. (2009). Global contour shapes are coded differently from their local components. *Vision Research, 49*(13), 1702–1710.

Bell, J., Sampasivam, S., McGovern, D., & Kingdom, F. A. A. (2010). More than a simple curve: Evidence for mechanisms which are selective for curves containing inflections. *Journal of Vision, 10*(7), 1163.

Bell, J., Wilkinson, F., Wilson, H. R., Loffler, G., & Badcock, D. R. (2009). Radial frequency adaptation reveals interacting contour shape channels. *Vision Research, 49*(18), 2306–2317.

Biederman, I. (1987). Recognition-by-components: A theory of human image understanding. *Psychological Review, 94*(2), 115–147.

Brincat, S. L., & Connor, C. E. (2004). Underlying principles of visual shape selectivity in posterior inferotemporal cortex. *Nature Neuroscience, 7*(8), 880–886.

Brincat, S. L., & Connor, C. E. (2006). Dynamic shape synthesis in posterior inferotemporal cortex. *Neuron, 49*(1), 17–24.

Carlson, E. T., Rasquinha, R. J., Zhang, K., & Connor, C. E. (2011). A sparse object coding scheme in area V4. *Current Biology, 21*(4), 288–293.

Connor, C. E. (2004). Shape dimensions and object primitives. In L. M. Chalupa & J. S. Werner (Eds.), *The visual neurosciences* (pp. 1080–1089). London: MIT Press.

Day, M., & Loffler, G. (2009). The role of orientation and position in shape perception. *Journal of Vision, 9*(10), 1–17.

De Winter, J., & Wagemans, J. (2006). Segmentation of object outlines into parts: A large-scale integrative study. *Cognition, 99*(3), 275–325.

Dickinson, J. E., Almeida, R. A., Bell, J., & Badcock, D. R. (2010). Global shape aftereffects have a local substrate: A tilt aftereffect field. *Journal of Vision, 10*(13), 5.

Field, D. J., Hayes, A., & Hess, R. F. (1993). Contour integration by the human visual system: Evidence for a local "association field". *Vision Research, 33*(2), 173–193.

Field, D. J., Hayes, A., & Hess, R. F. (2000). The roles of polarity and symmetry in the perceptual grouping of contour fragments. *Spatial Vision, 13*(1), 51–66.

Gheorghiu, E., & Kingdom, F. A. (2006). Luminance-contrast properties of contour-shape processing revealed through the shape-frequency after-effect. *Vision Research, 46*(21), 3603–3615.

Gheorghiu, E., & Kingdom, F. A. A. (2007a). Chromatic tuning of contour-shape mechanisms revealed through the shape-frequency and shape-amplitude after-effects. *Vision Research, 47*(14), 1935–1949.

Gheorghiu, E., & Kingdom, F. A. A. (2007b). The spatial feature underlying the shape-frequency and shape-amplitude after-effects. *Vision Research, 47*(6), 834–844.

Gheorghiu, E., & Kingdom, F. A. A. (2008). Spatial properties of curvature-encoding mechanisms revealed through the shape-frequency and shape-amplitude after-effects. *Vision Research, 48*(9), 1107–1124.

Gheorghiu, E., & Kingdom, F.A.A. (2009). Multiplication in curvature processing. *Journal of Vision, 9*(2) :23, 1-17.

Glass, L. (1969). Moire effect from random dots. *Nature, 223*(206), 578–580.

Habak, C., Wilkinson, F., & Wilson, H. R. (2006). Dynamics of shape interaction in human vision. *Vision Research, 46*(26), 4305–4320.

Habak, C., Wilkinson, F., Zakher, B., & Wilson, H. R. (2004). Curvature population coding for complex shapes in human vision. *Vision Research, 44*(24), 2815–2823.

Hancock, S., & Peirce, J. W. (2008). Selective mechanisms for simple contours revealed by compound adaptation. *Journal of Vision, 8*(7), 1–10.

Hayworth, K. J., & Biederman, I. (2006). Neural evidence for intermediate representations in object recognition. *Vision Research, 46*(23), 4024–4031.

Hess, R. F., Achtman, R. L., & Wang, Y. Z. (2001). Detection of contrast-defined shape. *Journal of the Optical Society of America A: Optics, Image Science, and Vision, 18*(9), 2220–2227.

Hess, R. F., Wang, Y. Z., & Dakin, S. C. (1999). Are judgements of circularity local or global? *Vision Research, 39*(26), 4354–4360.

Hoffman, D. D., & Richards, W. A. (1984). Parts of recognition. *Cognition, 18*(1–3), 65–96.

Hoffman, D. D., & Singh, M. (1997). Salience of visual parts. *Cognition, 63*(1), 29–78.

Jeffrey, B. G., Wang, Y. Z., & Birch, E. E. (2002). Circular contour frequency in shape discrimination. *Vision Research, 42*(25), 2773–2779.

Koenderink, J. J., & van Doorn, A. J. (1982). The shape of smooth objects and the way contours end. *Perception, 11*(2), 129–137.

Kourtzi, Z., & Kanwisher, N. (2001). Representation of perceived object shape by the human lateral occipital complex. *Science, 293*(5534), 1506–1509.

Kurki, I., Saarinen, J., & Hyvarinen, A. (2009). Integration of contour features into a global shape: A classification image study. *Perception, 38*, 25 (ECVP Abstract Supplement).

Lerner, Y., Hendler, T., Ben-Bashat, D., Harel, M., & Malach, R. (2001). A hierarchical axis of object processing stages in the human visual cortex. *Cerebral Cortex, 11*(4), 287–297.

Loffler, G. (2008). Perception of contours and shapes: Low and intermediate stage mechanisms. *Vision Research, 48*(20), 2106–2127.

Loffler, G., Wilson, H. R., & Wilkinson, F. (2003). Local and global contributions to shape discrimination. *Vision Research, 43*(5), 519–530.

Magnussen, S., & Kurtenbach, W. (1979). A test for contrast-polarity selectivity in the tilt aftereffect. *Perception, 8*(5), 523–528.

Motoyoshi, I., & Kingdom, F. A. A. (2010). The role of co-circularity of local elements in texture perception. *Journal of Vision, 10* (1):3, 1-8.

Mullen, K. T., & Beaudot, W. H. (2002). Comparison of color and luminance vision on a global shape discrimination task. *Vision Research, 42*(5), 565–575.

Mullen, K. T., Beaudot, W. H. A., & Ivanov, I. V. (2011). Evidence that global processing does not limit thresholds for RF shape discrimination. *Journal of Vision, 11*(3), 22.

Muller, K. M., Wilke, M., & Leopold, D. A. (2009). Visual adaptation to convexity in macaque area V4. *Neuroscience, 161*(2), 655–662.

Or, C. C.-F., Khuu, S. K., & Hayes, A. (2007). The role of luminance contrast in the detection of global structure in static and dynamic, same- and opposite-polarity, glass patterns. *Vision Research, 47*(2), 253–259.

Pasupathy, A., & Connor, C. E. (1999). Responses to contour features in macaque area V4. *Journal of Neurophysiology, 82*(5), 2490–2502.

Pasupathy, A., & Connor, C. E. (2001). Shape representation in area V4: Position-specific tuning for boundary conformation. *Journal of Neurophysiology, 86*(5), 2505–2519.

Pasupathy, A., & Connor, C. E. (2002). Population coding of shape in area V4. *Nature Neuroscience, 5*(12), 1332–1338.

Poirier, F. J. A. M., & Wilson, H. R. (2006). A biologically plausible model of human radial frequency perception. *Vision Research, 46*(15), 2443–2455.

Poirier, F. J. A. M., & Wilson, H. R. (2007). Object perception and masking: Contributions of sides and convexities. *Vision Research, 47*(23), 3001–3011.

Poirier, F. J. A. M., & Wilson, H. R. (2010). A biologically plausible model of human shape symmetry perception. *Journal of Vision, 10*(1), 1–16.

Wang, Y. Z., & Hess, R. F. (2005). Contributions of local orientation and position features to shape integration. *Vision Research, 45*(11), 1375–1383.

Wilkinson, F., James, T. W., Wilson, H. R., Gati, J. S., Menon, R. S., & Goodale, M. A. (2000). An fMRI study of the selective activation of human extrastriate form vision areas by radial and concentric gratings. *Current Biology, 10*(22), 1455–1458.

Wilkinson, F., Shahjahan, S., & Wilson, H. (2007). Hysteresis between shape-defined categories. *Journal of Vision, 7*(9), 209.

Wilkinson, F., Wilson, H. R., & Habak, C. (1998). Detection and recognition of radial frequency patterns. *Vision Research, 38*(22), 3555–3568.

Wilson, J. A., Switkes, E., & De Valois, R. L. (2004). Glass pattern studies of local and global processing of contrast variations. *Vision Research, 44*(22), 2629–2641.

Wilson, H. R., & Wilkinson, F. (2002). Symmetry perception: A novel approach for biological shapes. *Vision Research, 42*(5), 589–597.

Wilson, H. R., Wilkinson, F., Lin, L. M., & Castillo, M. (2000). Perception of head orientation. *Vision Research, 40*(5), 459–472.

Yamane, Y., Carlson, E. T., Bowman, K. C., Wang, Z., & Connor, C. E. (2008). A neural code for three-dimensional object shape in macaque inferotemporal cortex. *Nature Neuroscience, 11*(11), 1352–1360.

Yau, J., Pasupathy, A., Brincat, S., & Connor, C. (2010). Dynamic synthesis of curvature in area V4. *Journal of Vision, 10*(7), 911.